Study on appropriate heat mitigation technologies for urban block redevelopment based on demonstration experiments in Kobe city

Takebayashi, Hideki

Danno, Hiroki

Tozawa, Ushio

(Citation)
Energy and Buildings,250:111299

(Issue Date)
2021-11-01

(Resource Type)
journal article

(Version)
Accepted Manuscript

(URL)
https://hdl.handle.net/20.500.14094/90008588

Study on appropriate heat mitigation technologies for urban block redevelopment based on demonstration experiments in Kobe City

Hideki Takebayashi and Hiroki Danno, Department of Architecture, Graduate School of Engineering, Kobe University
Ushio Tozawa, Technical Management Division, Construction Bureau, Kobe City

Abstract

In order to promote the redevelopment of cities in consideration of measures against extreme heat, the effectiveness of various heat mitigation technologies introduced by Kobe City was evaluated. We introduced each technology for heat countermeasures to the central part of Kobe city, clarified their effects by measurement, and discussed issues and evaluations for the implementation. Watering on road, sunshade with mist spray, water surface, watering on pavement, and mist spray in a park were introduced, and their effects were evaluated using the thermal environment index SET* based on the measurement results. Since it is necessary to compare and evaluate multiple technologies, the thermal environment index of the human body was adopted as a common index. The reduction in surface temperature, MRT and SET* by watering on the roadway were about 10 °C, 1.9 °C and 0.8 °C, respectively, and the effects lasted for at least 30 minutes. SET* was greatly decreased when the upper fractal sunshade blocked solar radiation to the central measurement point under the sunshade. The reduction of MRT and SET* on the watered on the pavement were larger than that on the water surface because the watered area was larger than the water surface area. MRT reduction due to wetting of the globe ball sensor by the mist spray had a greater effect on SET* reduction than air temperature reduction due to evaporation of the mist.

Key words: urban heat island, extreme high temperature, watering on road, sunshade, mist spray, watering on pavement, water surface

Nomenclature

MRT: Mean Radiant Temperature (°C)
SET*: Standard New Effective Temperature (°C)
UHI: Urban Heat Island
WBGT: Wet Bulb Globe Temperature (°C)

1. Introduction

An effect produced by urban growth is the urban heat island (UHI), which is a phenomenon whereby the ambient temperature in cities is significantly higher than in rural areas due to an increase in artificial ground surfaces and artificial heat emissions. Mitigation measures such as green roofs, cool roofs, and water retaining materials, have been developed with the expectation that they will serve as countermeasures to the urban heat island [1-4]. In recent years, adaptive measures such as awnings, louvers, directional reflective materials, mist sprays, and evaporative materials have been developed as effective solutions to the outdoor human thermal environments under the influence of urban heat islands.

The effects of cool pavements are related to reflection, evaporation, and heat storage [5]. The effect of cool pavement is mainly obtained by reflection or evaporation, but the effect of evaporation is relatively promising because it is necessary to avoid the solar radiation reflected by the pavement from incident on the human body. Various studies have been conducted on cool pavement using evaporation as follows. The authors performed comparative surface heat budget measurements on several types of asphalt, concrete, and ceramic pavements developed in Japan, as well as soil and turf surfaces [6]. Cool pavements based on evaporation are classified as porous pavements, permeable pavements, and pervious pavements. In all cool pavements based on evaporation, the evaporation rate gradually decreases, and the cooling effect lasts only a few days after precipitation or watering. Relatively continuous evaporation can be expected in pavements with water retaining materials incorporated between porous aggregates, which are called water retaining pavements [6]. In addition, Akagawa et al. proposed the use of water retaining sheets using capillary action under the surface of the water retaining material in order to continue more continuous evaporation [7]. Watering on an as-needed basis or periodically is another possible alternative for continuous evaporation. Hendel et al. confirmed that watering reduced the surface temperature by 4 °C in the shade and 13 °C in the sun by infrared camera measurements [8]. Asaeda et al. focused on the heat storage and examined the heat budget on several kinds of pavements [9]. Qin and Hiller focused on the thermal inertia and examined the heat budget on the pavement surface [10]. The possibility of cooling benefits by irrigation was evaluated by Broadbent et al. [11]. Gao and Santamouris considered the temperature decrease due to irrigation and pointed out the necessity of optimizing irrigation in consideration of the relationship between irrigation cooling and the related factors [12]. The cooling effect of watering vegetation and irrigating pavement was analyzed by Daniel et al. [13]. Hendel et al. examined the optimization of the pavement-watering method [14]. They also examined the optimum watering method by paying attention to the sudden change in

surface temperature [8]. Wei and He examined a numerical simulation for analyzing the thermal improving effect of evaporative cooling on the urban surfaces [15].

Because of the administrative effort and cost involved in continuous irrigation and periodic watering, more strategic research is needed to realize cool pavements to improve outdoor human thermal environment. Several studies have already examined the improvement of outdoor human thermal environment by cool pavements as follows, but more practical studies are needed. Djekic et al. discussed the relationship between color, roughness, and shade of several materials and surface temperature and argued that the effects of sunshine and shade are dominant in human thermal comfort declaration based on the analysis of thermal comfort declaration survey [16]. Wang et al. reported that water sprinkling can reduce surface temperature and wet bulb globe temperature (WBGT) at a height of 0.5 m above cold pavement by up to 10 °C and 2 °C, respectively [17]. The authors also reported that the most dominant factor on the thermal environment of outdoor spaces is solar radiation shielding, followed by surface cover improvement [18]. They also state that solar radiation shielding by trees is necessary at least 10 meters from buildings on the south side and at least 6 meters from buildings on the east or west side [19]. In addition, based on the results of measurements and calculations in a large-scale redevelopment plaza in front of a major railway station, it has been discussed that the thermal environment design of outdoor spaces should be considered in the following order: shading by buildings, shading by trees, and improvement of surface materials [20].

Ulpiani organized the cooling effect of air temperature by mist spraying based on literature review [21]. They also clarified the decrease in temperature and UTCI by measurement, and examined the optimum operating conditions for mist spray [22]. Oh et al. evaluated an outdoor mist-spraying environment and its effect on thermal sensations, thermal environment, and skin temperature [23]. Desert et al. measured the spatial distribution of temperature and humidity around the mist spray and analyzed the relationship with human sensation and skin temperature [24]. These studies suggest that the effect of improving the thermal environment differs not only depending on the characteristics of the mist sprayer but also on the relationship with humans.

Kobe City has been studying and implementing specific measures targeting extreme high temperatures, based on its experience with recent abnormal summer temperatures (heat waves). In response to a request from the Kobe municipal government, the authors proposed measures for the city of Kobe based mainly on their findings. The authors reported on a study to derive strategies for dealing with extreme high temperatures based on thermal environment maps in street canyon [25]. In the summer of 2019, a

109 demonstration of cool spots in outdoor spaces was conducted, with fractal sunshades
110 spraying a fine mist of water on the plaza in front of a famous department store and on
111 the north-south street in front of a major train station [26]. In the summer of 2020, two
112 vehicles equipped with water tanks watered 32 tons of water on the roadway in an urban
113 area of about 25.8 hectares every day except for rainy days [27]. Figure 1 shows the flow
114 chart of this study, showing objective sites, measurement, evaluation, and discussion of
115 each technology. By using the thermal environment index of the human body as a
116 common index, it is possible to compare countermeasure technologies by different
117 mechanisms. Since it is premised on the application of various technologies to the real
118 society, the effect of the watered lane, the time change of solar shading, the effects of the
119 watered width and the distance to the human body were presented as points of discussion.
120 The following studies have been conducted as comprehensive studies related to the urban
121 thermal environment. Parker clarified the characteristics of the urban heat island in
122 Leeds, UK and integrated it with the building energy simulation [28]. Congedo and
123 Baglivo proposed the Apulia ITACA Protocol, which comprehensively evaluates various
124 environmental performances at the district level [29]. It also covers the thermal
125 environment of the outdoor space, which is the subject of this study, but is an integrated
126 tool for a wider range of environmental issues such as LEED. In the case study in small
127 district of Lecce, Italy by Congedo et al., the heat island effect was also evaluated as one
128 of many environmental indicators [30]. Degirmenci et al. discussed the policy and
129 technology responses to mitigating the effects of UHIs based on literature reviews. They
130 pointed out that the policy and technology response to UHI was considered separately,
131 but lacked the integration of combined interventions [31]. The effects of local climate
132 change on energy consumption and public health were comprehensively evaluated by
133 Santamouris, M. [32]. The possibility of reducing ambient temperature by several kinds
134 of local climate mitigation technologies was evaluated by M. Santamouris et.al. [33].
135 In this study, the effects of various heat mitigation technologies introduced by Kobe City
136 were evaluated in order to promote urban redevelopment in consideration of measures
137 against extreme heat. The challenge is to implement measures against heat in the real
138 society based on the characteristics of each technology. This study aims to make better
139 technology useful in the real society. We introduced each technology for heat
140 countermeasures to the central part of Kobe city, clarified their effects by measurement,
141 and discussed issues and evaluations for the implementation. Since it is necessary to
142 compare and evaluate multiple technologies, the thermal environment index of the
143 human body was adopted as a common index. Although each technology was evaluated
144 individually in the previous study, this study comprehensively discusses how to

implement countermeasures appropriately in the real society.

2. Outline of the measurement

Kobe city is located on Osaka Bay. The climate is classified as a warm temperate climate; according to Köppen and Geiger, this climate is classified as Cfa. The average annual temperature is 16.7 °C. The average annual rainfall is 1,216 mm. 32 tons/day of water watered on an urban area of about 25.8 ha is equivalent to 310 kJ/(m^2day) (32,000 [kg/day] × 2,500 [kJ/kg] / 258,000 [m^2] = 310 [kJ/(m^2day)], the latent heat of water vaporization was assumed to be 2,500 [kJ/kg]), which is 1.24 % of the daily integrated solar radiation of about 25 MJ/(m^2day) on a clear summer day. Watering was carried out by two vehicles equipped with water tanks, with the route set to cover the entire target area.

Air temperature, relative humidity, surface temperature, wind direction and velocity, globe temperature, solar radiation, and thermal images were measured at each measurement point using a thermistor, capacitive humidity sensor, infrared thermometer, windsock, hot wire anemometer, 15 cm diameter globe ball, pyranometer, and thermal camera. An overview of the measuring instruments and their settings are shown in Table 1 and Figure 2. The measurer moved to the measurement points with the cart shown in Figure 2 and the portable measuring instruments (infrared thermometer, windsock, hot wire anemometer, and thermal camera).

The measurement points are shown in Figure 3. "Sunshade-1" and "Sunshade-2" are "b. sunshade on sidewalk" and "Mist spray" is "d. mist spraying in park" in Figure 1. "Water surface" and "Watering pavement" are "c. water surface and pedestrian passage" in the same park. Two vehicles equipped with water tanks performed "a. watering on roadway" and continuous measurements were carried out at each measurement point just before and 30 minutes after the watering. "NS-L", "NS-M", and "NS-S" are the measurement points on north-south roads with large, medium, and small road widths. "NS-WR" is a measurement point on a north-south road with water retaining pavement. "EW-L", "EW-M", and "EW-S" are measurement points on east-west roads with large, medium, and small road widths. Measurements were also taken at the crossroads "CROS" and at the reference point "REF". All measurements were taken by the same instruments on typical sunny summer days, but not on the same date and time.

3. Measurement results

In this chapter, the measurement results and Evaluation by MRT, SET* of 1) watering on road, 2) sunshade with mist spray, 3) water surface and watering on pavement in a

park, 4) mist spray in a park of are explained according to the flowchart shown in Figure 1.

3.1 Watering on road

Measurements were taken on July 30 and August 5, 2020, from 9:00 to 11:00 and from 13:00 to 15:00. Air temperature, relative humidity, wind direction and velocity, and surface temperature on the watered roadway were measured immediately before and after the water supply, and every 5 minutes until 30 minutes later. Since only one of the multiple lanes was watered, no decrease in air temperature or increase in relative humidity was observed in the measurements at a height of 1.2 meters. Wind direction tended to follow the road, and wind velocity tended to be higher on the wider road, which was not affected by the water supply. Measurement results of the difference in road surface temperature with and without watering immediately after and 30 minutes after watering are shown in Figure 4. The horizontal axis is surface temperature without watering, and the vertical axis is the difference between surface temperature without and with watering. The left sides are immediately after watering, and the right sides are 30 minutes after watering. The upper sides are on north-south road, and the lower sides are on east-west road. White symbols are in shade, colored symbols are in sun. The effect of watering was greater the higher the surface temperature on the un-watered road during sunny condition. The maximum decrease in surface temperature was about 10 °C. The relationship between the horizontal and vertical axes is not significantly different between the left graph and the right graph, which means that the effect of watering lasted for at least 30 minutes. The relationship between the effect of watering and the direction and width of the road could not be confirmed. Since the water was supplied to the roadway near the center of the road, the shadows cast by the surrounding buildings did not have a significant effect on the surface temperature measurement results for any orientation and width of the road.

At each measurement point, the view factor between the surrounding objects and the measurement point is read from the image captured by the camera using a fisheye lens. Figure 5 shows the view factor for each measurement point. The surface cover around the measurement point was divided into watered roadway in the vicinity, sidewalk just below, roadway and sidewalk on the other side, near wall, far wall and sky. Since the measurement point was set at the boundary between the roadway and the sidewalk, the view factor of watered roadway is almost 0.2. Figure 6 shows Mean Radiant Temperature (MRT) difference between the roadway with and without watering just after watering and 30 minutes after watering. The horizontal axis is MRT without watering, and the vertical axis is the difference between MRT without and with watering. The left sides

are immediately after watering, and the right sides are 30 minutes after watering. The upper sides are on north-south road, and the lower sides are on east-west road. Reflecting the maximum surface temperature difference of 10 °C and the view factor of 0.2 for the watered roadway, the maximum MRT difference is about 2 °C. The relationship between the horizontal and vertical axes of the MRT is not as clear as that of the surface temperature, because the MRT is affected by the view factor of 0.8, excluding watered roads, and solar radiation directly incident on the human body. Standard New Effective Temperature (SET*) was calculated using the calculated MRT and the measured values of air temperature, relative humidity, and wind velocity at each measurement point. The amount of clothing and metabolic rate were assumed to be 0.6 clo (1 clo = 0.155 Km^2/W) and 1.4 met (1 met = 58.2 W/m^2), respectively. The SET* difference between the roadway with and without watering just after watering and 30 minutes after watering is shown in Figure 7. The horizontal axis is SET* without watering, and the vertical axis is the difference between SET* without and with watering. The left sides are immediately after watering, and the right sides are 30 minutes after watering. The upper sides are on north-south road, and the lower sides are on east-west road. The maximum difference in SET* is about 0.8° C. It can be seen that the solar radiation directly incident on the human body is quite dominant to the SET* via MRT.

3.2 Sunshade with mist spray

The sunshade was fractal-shaped [34], 2 m × 4 m in size, 2.5 m in height, mist sprays were installed on four square columns at a height of 1.5 m. Measurements were taken on July 30 and August 5, 2019 from 10:00 to 17:00. Mist was sprayed from 11:00 to 15:00. Air temperature, relative humidity, globe temperature, and solar radiation at the center under the sunshade were measured every 5 seconds using a data logger. In addition, the wind direction and velocity under the sunshade and the surface temperature of representative surface materials were measured hourly by the measurer. The same measurements were carried out at reference points set in the immediate vicinity of each sunshade. Measurement results of air temperature and absolute humidity on July 30, 2019 are shown in Figure 8. Red line is under the sunshade, blue line is the reference point without sunshade. The upper sides are measurement results of air temperature, and the lower sides are measurement results of absolute humidity. The left sides are under sunshade-1, and the right sides are under sunshade-2. The measurement results on August 5 were similar to those on July 30. Air temperature under the sunshade was lower than the nearby reference point without the sunshade, but the absolute humidity showed little difference between the two points with and without the sunshade. The

sprayed mist did not directly affect the air temperature and humidity sensors, but the decrease in surface temperature and solar radiation shielding affected the decrease in air temperature. The calculated results of SET* under the sunshade-1 and -2 and nearby reference points without sunshade on July 30, 2019 are shown in Figure 9. Blue lines are sunshade-1, red lines are sunshade-2. Dashed lines are under the sunshade, dotted lines are the reference points without sunshade. SET* was calculated using the measured air temperature, relative humidity, wind velocity, and MRT calculated from the measured surface temperature and solar radiation. The amount of clothing and metabolic rate were assumed to be 0.6 clo and 1.4 met, respectively. Sunshade-1 was located on the north-south road, so it was shaded by the surrounding buildings before 10:00 and after 14:00. Sunshade-2 was located in an open space, so it was shaded by the surrounding buildings only after 16:00. The large decrease in SET* from 11:00 to 13:00 was due to the fractal sunshade at the top blocking solar radiation to the central measurement point under the sunshade. Outside of this time period, there was little difference between SET*s with and without the sunshade. The shielding of solar radiation to the measurement point is quite dominant for the SET*.

3.3 Water surface and watering on pavement in a park

Running water is artificially circulated in a canal in the park. The location of the measurement points on the water surface are shown in Figure 10. The measurement point for pedestrians was set in the center of a 7.5 m pedestrian passage. The measurements were taken from 11:00 to 17:00 on August 13, 2020. Air temperature, relative humidity, wind direction and velocity, globe temperature, solar radiation, and surface temperature on water surface, pavements, walls, and plants were measured hourly. MRT and SET* on the water surface and its surroundings on August 13, 2020 are shown in Figure 11. Left side is MRT, right side is SET*. Blue line is on water surface, red line is nearby water surface, gray line is on pedestrian passage. MRT was calculated from the view factors based on the fisheye photographs and surface temperature measurements. SET* was calculated using the calculated MRT and air temperature, relative humidity, and wind velocity measured at each measurement point. The amount of clothing and metabolic rate were assumed to be 0.6 clo and 1.4 met, respectively. At all measurement points, MRT and SET* were higher during the day when solar radiation was higher, but MRT and SET* on the water surface were about 1.8 °C and 1.1 °C lower on average than those on the pedestrian passage. This is because the surface temperature difference between the water surface and the pedestrian passage is relatively large, about 15 °C. As the pedestrians approached the water surface, MRT and

SET* were almost the same as on the water surface.

The watering experiment was conducted by watering 2 m width on the same pedestrian pavement in the park. As with watering on the roadway, a sufficient amount of water was supplied to completely wet the surface. Measurements were taken on August 12, 2020, from 8:00 to 8:30 and from 14:00 to 14:30. Air temperature, relative humidity, wind direction and velocity, and surface temperature on the watered pavement surface and its surroundings were measured immediately before and after watering, and every 5 minutes until 30 minutes later. MRT and SET* on pedestrian passage with and without watering before watering to 30 minutes after watering are shown in Figure 12. Blue line is on pavement with watering, red line is on pavement without watering. Upper sides are MRT, lower sides are SET*. Left sides are at 8:00, right sides are at 14:00. MRT and SET* were calculated in the same way as above. MRT and SET* on the pedestrian passage with watering were about 1.3 °C, 4.0 °C and 0.9 °C, 2.5 °C lower on average at 8:00 and 14:00, respectively, compared to those on the pedestrian passage without watering. These effects were obtained because the view factor of the 2 m wide watered pavement was larger than that of the 1 m wide water surface, although the maximum reduction on pavement surface temperature due to watering was 10 °C, which was smaller than on water surface (15°C).

3.4 Mist spray in a park

Wooden flowerbeds and benches were placed in the park, in which the mist spray outlets and associated pumps and pipes are hidden. The location of the measurement points placed in front of the mist spray outlets is shown in Figure 13. The mist spray outlet was installed at 1.3 m above the ground. As shown in Figure 13, enough water is supplied to wet the tile surface under shaded conditions. The measurement points were set near and slightly away from the mist outlets. The measurements were carried out from 10:00 to 11:00 and from 16:00 to 17:00 on August 12, 2020. At each measurement point, air temperature, relative humidity, wind direction and velocity, globe temperature, and surface temperature on surrounding materials were measured in 15 minutes. Measurement results of globe temperature in front of mist sprays are shown in Table 2. Air temperature decreased by about 1 °C and relative humidity increased by about 1 % at 30 cm from the mist outlet. It was observed that there was a large difference in globe temperature. In the shade, the differences were 4.3 °C and 2.6 °C before noon and in the evening, respectively. In the sun, the differences were 19.4 °C and 10.2 °C before noon and in the evening, respectively. The globe ball that the temperature sensor put inside at 30 cm from the mist outlet got wet, but the globe balls at 130 cm and 230 cm from the

mist outlets did not. Globe temperature differences at 30 cm and 130, 230 cm from the mist outlet corresponds to 115 W/m^2 and 68 W/m^2 of evaporation heat in the shade, and 520 W/m^2 and 226 W/m^2 of evaporation heat in the sun. This means that when the human body is wetted by mist spray, the effect of improving the thermal sensation is significant. MRT and SET* in front of mist spray are shown in Table 3. MRT takes into account the effect of wet globe balls. SET* is calculated using measured air temperature, relative humidity, wind velocity, MRT calculated above, and solar radiation. The reduction in MRT due to wetting of the globe ball had a greater effect on the reduction in SET* than the reduction in air temperature due to evaporation of the mist.

4. Discussion

Since it is premised on the application of various technologies to the real society, 1) the effect of watered lane on human thermal sensation, 2) time change in the effect of sunshade, 3) the effects of watered width and distance to human body on human thermal sensation are presented as points of discussion. In this chapter, these discussions are carried out and guidelines for future urban redevelopment are examined.

4.1 Effect of watered lane on human thermal sensation

From the measurement results, the maximum reduction in surface temperature by watering road was about 10 °C, and the effect lasted for at least 30 minutes. However, the improvement in the human thermal sensation is affected by the distance from the watered lane to the human body. Distance from watered lane to the human body and SET* reduction when the watered lane is changed is shown in Figure 14. The horizontal axis is the distance from watered lane to the human body, and the vertical axis is SET* reduction by watering roadway. Image of the view factor between human body and watered lane is shown on the right side. The image of the road side and parking zone between the first lane and the sidewalk is shown below the figure. Then, SET* reduction when the road side and parking zone are available is indicated by the white arrow in the figure. The width of a lane was assumed to be 3 m, which is the general width of the roadway. SET* reduction is shown when the road surface temperature decreases by 5, 10, 15, and 20 °C due to watering, and 10.6, 7.4 °C which are the maximum measured values immediately after watering and 30 minutes later, respectively. The smaller the reduction in surface temperature and the greater the distance from the watered lane to the human body, the smaller the reduction in SET*. When water is supplied on the first and second lanes, the SET* reduction is about 0.48 °C and 0.07 °C, respectively, assuming the surface temperature reduction is 10.6 °C. In reality, there may be a road side or parking zone between the sidewalk and the roadway. In such cases, SET*

decreases from 0.48 °C to 0.34 °C and 0.12 °C, respectively. Furthermore, pedestrians may walk away from the roadway. When a pedestrian walks 1 meter away from the roadway, the reduction in SET* decreases from 0.48 °C to 0.24 °C. Watering in the first lane and pedestrians walking beside it are key points to improve pedestrians' thermal sensation.

4.2 Change with time in the effect of sunshade with mist spray

From the measurement results, SET* was greatly decreased when the upper fractal sunshade blocked solar radiation to the central measurement point under the sunshade. However, outside of this time period, there was little difference between SET*s with and without the sunshade. Therefore, time variation of shade by the sunshade is important for improving thermal sensation. The effect of the mist spray was hardly observed. Changes with time in solar radiation shade by sunshades and roadside trees are shown in Figure 15. The red line shows the shade by time. Upper sides are shade by sunshades with 2 m × 4 m, 2.5 m high, lower sides are shade by roadside trees with 10 m high. Left sides are on north-south road, right sides are on east-west road. In the case of sunshades on the north-south road sidewalk, the sunshade is effective on the western sidewalk in the morning and on the eastern sidewalk in the afternoon. However, the shadow directly under the sunshade is limited to before and after noon. Vertical louvers, blinds, etc. are required to ensure the effect on the directly under the sunshade. In the case of sunshades on the east-west road sidewalk, the sunshade is effective on the northern sidewalk, but it is not effective on the southern sidewalk. In the case of roadside trees on the north-south road sidewalk, the sunshade is effective on a relatively wide area, but it is limited in morning or evening on either sidewalk. In the case of roadside trees on the east-west road sidewalk, the sunshade is effective along the sidewalk. From the above, it is necessary to consider the distance in the east-west direction when arranging sunshades and trees in order to obtain the effect of solar radiation shielding over a wide area. On the other hand, if sunshades and trees are arranged in the east-west direction, a space against extreme heat will be formed.

4.3 Effect of watered width and distance to human body on human thermal sensation

From the measurement results, the maximum reduction in surface temperature by water surface and watering pavement was about 15 °C and 10 °C, respectively. Distance from watered surface to the human body and view factor, MRT reduction is shown in Figure 16. The horizontal axis is the distance from watered surface to the human body, and the vertical axis is view factor between watered surface and human body. Colored

lines indicate the watered width. MRT reduction is calculated as the product of the view factor and the surface temperature reduction as shown in table in Figure 15. When the pedestrian is on the water surface, MRT reduction is large because the view factor is large. But when the pedestrian is on the passage beside the water surface, MRT reduction is small because the view factor is small even if the width of the water surface is 2 m. Even on the passage away from the water surface, if water is supplied at the foot of the pedestrian with a width of 2 m, MRT reduction is similar to that on the water surface. It is hard to reconstruct the water surface with a specific water depth and flow rate in the park. On the other hand, watering on the pavement is relatively easy to manage in terms of location, time, and amount of water supplied.

4.4 Summary of the effects of improving the human thermal sensation and examination of the guidelines for future urban redevelopment

We evaluated the effects of watering on the roadway, sunshade with mist spray, water surface, watering on the pavement and mist spray in a park on improving the human thermal sensation. Table 4 shows a summary of the effects on the improvement of human thermal sensation.

By watering on the roadway when the surface temperature was above 40 °C, the maximum reduction in surface temperature, MRT and SET* were about 10 °C, 1.9 °C and 0.8 °C, respectively. In the cases of watering on the first and second lanes, MRT reduction were about 1.6 °C and 0.25 °C, respectively, and SET* reduction were about 0.5 °C and 0.07 °C, respectively, even though surface temperature reduction is the same at 10 °C, resulting in large differences in MRT and SET*.

When the incident solar radiation to the human body was shielded by the sunshade, the reduction in MRT and SET* were about 15 °C and 7 °C, respectively. The effect of street tree was similar to that of the sunshade. However, the effect of the sunshade and street tree do not always improve the thermal sensation in the lower and surrounding space throughout the day. The plan for installing the sunshade and street tree should take into account the temporal change in solar radiation shielding.

The reduction of surface temperature by the water surface in a park was about 15 °C, which was larger than that by watering on the pavement. However, the reduction of MRT and SET* at the center of the sidewalk 3.75 m away from the water surface was about 0.2 °C and 0.1 °C, respectively. In this table, the reduction of MRT and SET* on the watered on the pavement were larger than that on the water surface because the watered area was larger than the water surface area.

Air temperature decrease and relative humidity increase in the vicinity of the mist

outlets were about 1 °C and 1 %, respectively. When the human body got wet, MRT and SET* decreases were large, ranging from 2.9 to 19.4 °C, and 1.2 to 8.2 °C, respectively. In situations where it is acceptable for the human body to be wetted by the mist spray, such as in recreational areas, the effect of improving the thermal sensation can be expected.

As shown in Table 4, the improvement of human thermal sensation varies depending on the distance from the countermeasure technologies to the human body. Based on the characteristics of the target space, each technology should be selected appropriately in consideration of the following points. Regarding mist spray, is it acceptable for mist to wet the human body? Regarding water surface, is it acceptable to have a walking space on the water surface? Regarding watering pavement, is it acceptable that the pavement underfoot is wet? Regarding watering road, is it possible to supply water up to the edge of the road? Regarding street trees, is it possible to maintain the trees, such as pruning? Regarding sunshade, is it possible to match the shade area with the location of visitors?

5. Conclusion

We introduced each technology for heat countermeasures to the central part of Kobe city, clarified their effects by measurement, and discussed issues and evaluations for the implementation. Since it is necessary to compare and evaluate multiple technologies, the thermal environment index of the human body was adopted as a common index. Since it is premised on the application of various technologies to the real society, the effect of the watered lane, the time change of solar shading, the effects of the watered width and the distance to the human body were presented as points of discussion. Then, guidelines for future urban redevelopment were examined using the effects of improving human thermal sensation.The reduction in surface temperature, MRT and SET* by watering on the roadway were about 10 °C, 1.9 °C and 0.8 °C, respectively, and the effects lasted for at least 30 minutes. SET* was greatly decreased when the upper fractal sunshade blocked solar radiation to the central measurement point under the sunshade. Surface temperature reduction by water surface and watering on the pavement was about 15 °C and 10 °C, respectively. The reduction of MRT and SET* on the watered on the pavement were larger than that on the water surface because the watered area was larger than the water surface area. MRT reduction due to wetting of the globe ball sensor by the mist spray had a greater effect on SET* reduction than air temperature reduction due to evaporation of the mist.

Currently, Kobe City is considering the redevelopment of the city center, including the main station, city hall and several civic service functions, as well as the areas around

the sub-main train stations, in consideration of measures against extreme heat. Based on the results of this study, we will be discussing with the engineers of the various departments of the city on measures to deal with extreme heat.

Funding: This research was supported by Kobe city.
Acknowledgments: The authors thank Mr. Toshiyuki Sano and others of Kobe city for their cooperation.
Conflicts of Interest: The authors declare no conflicts of interest.

References

[1] Akbari, H.; Kolokotsa, D. Three decades of urban heat islands and mitigation technologies research. Energy Build. 2016, 133, 834–842. 10.1016/j.enbuild.2016.09.067
[2] Aleksandrowicz, O.; Vuckovic, M.; Kiesel, K.; Mahdavi, A. Current trends in urban heat island mitigation research: Observations based on a comprehensive research repository. Urban Clim. 2017, 21, 1–26. 10.1016/j.uclim.2017.04.002
[3] Santamouris, M. Cooling the cities—A review of reflective and green roof mitigation technologies to fight heat island and improve comfort in urban environments. Sol. Energy 2014, 103, 682–703. 10.1016/j.solener.2012.07.003
[4] Santamouris, M. Using cool pavements as a mitigation strategy to fight urban heat island—A review of the actual developments. Renew. Sustain. Energy Rev. 2013, 26, 224–240. 10.1016/j.rser.2013.05.047
[5] Qin, Y. A review on the development of cool pavements to mitigate urban heat island effect, Renew. Sustain. Energy Rev. 2015, 52, 445-459, 10.1016/J.RSER.2015.07.177
[6] Takebayashi, H.; Moriyama, M. Study on surface heat budget of various pavements for urban heat island mitigation. Advances in Materials Science and Engineering 2012, 10.1155/2012/523051
[7] Akagawa, H.; Komiya, H. Experimental study on pavement system with continuous wet surface. Journal of Architecture, Planning and Environmental Engineering (Transactions of AIJ) 2000, 530, 79-85.
[8] Hendel, M.; Colombert, M.; Diab, Y.; Royon, L. Improving a pavement-watering method on the basis of pavement surface temperature measurements. Urban Climate 2014, 10, 1, 189-200, 10.1016/j.uclim.2014.11.002
[9] Asaeda, T.; Ca, V.; Wake, A. Heat storage of pavement and its effect on the lower atmosphere. Atmos. Environ. 1996, 30, 3, 413-427, 10.1016/1352-2310(94)00140-5
[10] Qin, Y.; Hiller, J. Understanding pavement-surface energy balance and its implications on cool pavement development. Energy and Buildings 2014, 85, 389–399,

505 10.1016/j.enbuild.2014.09.076
506 [11] Broadbent, A.M.; Coutts, A.M.; Tapper, N.J.; Demuzere, M. The cooling effect of
507 irrigation on urban microclimate during heatwave conditions, Urban Clim. 2018, 23,
508 309-329, 10.1016/j.uclim.2017.05.002
509 [12] Gao, K.; Santamouris, M. The use of water irrigation to mitigate ambient
510 overheating in the built environment: Recent progress, Build. Environ. 2019, 164.
511 10.1016/j.buildenv.2019.106346
512 [13] Daniel, M.; Lemonsu, A.; Viguié V. Role of watering practices in large-scale urban
513 planning strategies to face the heat-wave risk in future climate. Urban Clim. 2018, 23.
514 10.1016/j.uclim.2016.11.001
515 [14] Hendel, M.; Colombert, M.; Diab, Y.; Royon, L. An analysis of pavement heat flux to
516 optimize the water efficiency of a pavement-watering method. Appl. Therm. Eng. 2015,
517 78, 658-669. 10.1016/j.applthermaleng.2014.11.060
518 [15] Wei, J.; He, J. Numerical simulation for analyzing the thermal improving effect of
519 evaporative cooling urban surfaces on the urban built environment. Appl. Therm. Eng.
520 2013, 51, 144-154. 10.1016/j.applthermaleng.2012.08.064
521 [16] Djekic, J.; Djukic, A.; Vukmirovic, M.; Djekic, P.; Brankovic, M. Thermal comfort of
522 pedestrian spaces and the influence of pavement materials on warming up during
523 summer. Energy and Buildings 2018, 159, 474-485, 10.1016/j.enbuild.2017.11.004
524 [17] Wang, J.; Meng, Q.; Tan, K.; Zhang, L.; Zhang, Y. Experimental investigation on the
525 influence of evaporative cooling of permeable pavements on outdoor thermal
526 environment. Building and Environment 2018, 140, 184-193,
527 10.1016/j.buildenv.2018.05.033
528 [18] Takebayashi, H.; Kyogoku, S. Thermal environmental design in outdoor space
529 focusing on radiation environment influenced by ground cover material and solar
530 shading, through the examination on the redevelopment buildings in front of central
531 Osaka station. Sustainability 2018, 10, 337, doi:10.3390/su10020337
532 [19] Takebayashi, H.; Kasahara, M.; Tanabe, S.; Kouyama, M. Analysis of solar radiation
533 shading effects by trees in the open space around buildings. Sustainability 2017, 9, 1398,
534 doi:10.3390/su9081398
535 [20] Takebayashi, H. Thermal environment design of outdoor spaces by examining
536 redevelopment buildings opposite central Osaka station. Climate 2019, 7, 143,
537 doi:10.3390/cli7120143
538 [21] Ulpiani, G. Water mist spray for outdoor cooling: A systematic review of technologies,
539 methods and impacts. Appl. Energy 2019, 254. 10.1016/j.apenergy.2019.113647
540 [22] Ulpiani, G.; Giuseppe, E.; Perna, C.; D'Orazio, M.; Zinzi, M. Thermal comfort

541 improvement in urban spaces with water spray systems: Field measurements and survey.
542 Build. Environ. 2019, 156, pp. 46-61, 10.1016/j.buildenv.2019.04.007
543 [23] Oh, W.; Ooka, R.; Nakano, J., Kikumoto, H.; Ogawa, O. Evaluation of mist-spraying
544 environment on thermal sensations, thermal environment, and skin temperature under
545 different operation modes. Build. Environ. 2020, 168. 10.1016/j.buildenv.2019.106484
546 [24] Desert, A.; Naboni, E.; Garcia, D. The spatial comfort and thermal delight of outdoor
547 misting installations in hot and humid extreme environments. Build. Environ. 2020, 224.
548 10.1016/j.enbuild.2020.110202
549 [25] Takebayashi, H.; Okubo, M.; Danno, H. Thermal environment map in street canyon
550 for implementing extreme high temperature measures. Atmosphere 2020, 11, 550,
551 doi:10.3390/atmos11060550
552 [26] The Kobe Shimbun. What is the effect of artificial shade? Kobe city's proof
553 experiment for high temperature measures in the city center. Available online:
554 https://www.kobe-np.co.jp/news/sougou/201907/0012478089.shtml (accessed on 24
555 December 2020). (In Japanese)
556 [27] The Kobe Shimbun. 32 tons a day, cool the city every day by watering trucks in
557 central Kobe city. Available online: https://www.kobe-
558 np.co.jp/news/sougou/202008/0013596657.shtml (accessed on 24 December 2020). (In
559 Japanese)
560 [28] Parker, J.; The Leeds urban heat island and its implications for energy use and
561 thermal comfort. Energy and Buildings 2021, 235. doi:10.1016/j.enbuild.2020.110636.
562 [29] Congedo, P. M., Baglivo, C.; Implementation hypothesis of the Apulia ITACA
563 Protocol at district level – part I: The model. Sustainable Cities and Society 2021, 70.
564 doi:10.1016/j.scs.2021.102931.
565 [30] Congedo, P. M., Baglivo, C., Toscano, A. M.; Implementation hypothesis of the Apulia
566 ITACA Protocol at district level – part II: The case study. Sustainable Cities and Society
567 2021, 70. doi:10.1016/j.scs.2021.102927.
568 [31] Degirmenci, K., Desouza, K. C., Fieuw, W., Watson R. T., Yigitcanlar, T.;
569 Understanding policy and technology responses in mitigating urban heat islands: A
570 literature review and directions for future research. Sustainable Cities and Society 2021,
571 70. doi:10.1016/j.scs.2021.102873.
572 [32] Santamouris, M. Recent progress on urban overheating and heat island research.
573 Integrated assessment of the energy, environmental, vulnerability and health impact.
574 Synergies with the global climate change. Energy Build. 2020, 207.
575 10.1016/j.enbuild.2019.109482
576 [33] Santamouris, M.; Paolini, R.; Haddad, S.; Synnefa, A.; Garshasbi, S.; Hatvani-

Kovacs, G.; Gobakis, K.; Yenneti, K.; Vasilakopoulou, K.; Feng, J.; Gao, K.; Papangelis, G.; Dandou, A.; Methymaki, G.; Portalakis, P.; Tombrou, M. Heat mitigation technologies can improve sustainability in cities an holistic experimental and numerical impact assessment of urban overheating and related heat mitigation strategies on energy consumption, indoor comfort, vulnerability and heat-related mortality and morbidity in cities. Energy Build. 2020, 217. 10.1016/j.enbuild.2020.110002

[34] Sakai, S.; Nakamura, M.; Furuya, K.; Amemura, N.; Onishi, M.; Iizawa, I.; Nakata, J.; Yamaji, K.; Asano, R.; Tamotsu, K. Sierpinski's forest: New technology of cool roof with fractal shapes. Energy and Buildings 2012, 55, 28-34. j.enbuild.2011.11.052.

588 Table 1 Overview of the measuring instruments

Measurement instrument	Sensor (Manufacturer, Model)	Method, accuracy
Air temperature	Thermistor (Espec, RS-14)	Every 5 seconds, ±0.5 °C
Relative humidity	Capacitive humidity sensor (Espec, RS-14)	Every 5 seconds, ±5 %
Surface temperature	Infrared thermometer (Daiichisyoji, UT-02)	Average of several samplings, ±1 %
Wind direction	Windsock (self-made)	Most frequent in the period
Wind velocity	Hot wire anemometer, (Kanomax, 6036)	Average of 30 measurements, ±3 % or 0.015 m/s
Globe temperature	Globe ball (Eikoseiki, diameter 15 cm)	Every 5 seconds, ±0.3 °C
Solar radiation	Pyranometer (Tsuruga Electric, LP PYRA03)	Every 5 seconds, ±25 W/m^2
Thermal image	Thermal camera (FLIR Systems, FLIR ONE)	Measure the area around the measurement point

589

590 Table 2 Measurement results of globe temperature in front of mist sprays on August 12

	10:00-11:00	16:00-17:00	Condition
30 cm from mist outlet on tile surface [°C]	34.7	28.8	Shade
130 cm from mist outlet on tile surface [°C]	39.0	31.4	
Difference between 30 cm and 130 cm[°C]	4.3	2.6	
Equivalent evaporative heat [W/m^2]	115	68	
30 cm from mist outlet on grass surface [°C]	27.6	32.1	Sunny
230 cm from mist outlet on grass surface [°C]	47.0	42.3	
Difference between 30 cm and 230 cm [°C]	19.4	10.2	
Equivalent evaporative heat [W/m^2]	520	226	

591

592 Table 3 MRT and SET* in front of mist sprays on August 12

	10:00 - 11:00		16:00 - 17:00	
	MRT [°C]	SET* [°C]	MRT [°C]	SET* [°C]
30 cm from mist outlet on tile surface	34.9	28.5	28.2	24.1
130 cm from mist outlet on tile surface	40.1	31.3	31.1	26.2
30 cm from mist outlet on grass surface	27.6	23.5	31.8	29.0
230 cm from mist outlet on grass surface	47.0	39.5	42.9	38.2

593

Table 4 Summary of the effects on the improvement of human thermal sensation

	Surface temp. reduction	MRT reduction	SET* reduction	Condition
Watering on road	10 °C[*1]	1.9 °C	0.8 °C	Watering on First lane and pedestrian is beside it
		0.25 °C	0.07 °C	Watering on Second lane and pedestrian is beside it
Sunshade	-	15 °C	7 °C	When human body is shaded
Water surface	15 °C	0.2 °C	0.1 °C	On passage 3.75 m away
		1.6 °C	1.2 °C	On 1 m wide water surface
Watering on pavement	5 - 10 °C	1.3 - 4.0 °C	0.9 - 2.5 °C	On passage with 2 m width watered
Mist spray	-[*2]	2.9 - 19.4 °C	1.2 - 8.2 °C	When human body gets wet
Street tree[*3]	17.4 °C	16.1 °C	6.8 °C	When human body and ground surface is shaded

*1: When the surface temperature before watering exceeds 40 °C.

*2: The decrease in air temperature and increase in relative humidity in the vicinity of the mist outlets were about 1 °C and 1 %, respectively.

*3: From measurement results in Kobe City.

Figures list:




Sites	Watering on roadway	Sunshade on sidewalk	Water surface and pedestrian passage	Mist spraying in park
Measurment points	On east-west and north-south roads with large, medium, small road widths, crossroad with and without watering	Under fractal-shaped sunshade with 2m × 4m, 2.5m high, mist sprays on four corner columns at 1.5 m high	On and nearby water surface, pedestrian passage with and without watering	30, 130, 230 cm from mist outlet on tile and grass surface
Measurement elements	Air temperature, relative humidity, globe temperature, solar radiation, wind direction, wind velocity, surface temperature, view factor			
Evaluation indices	MRT and SET*			
Points of discussion	Effects of watered lane on human thermal sensation	Change with time in the effect of sunshade with mist spray	Effect of watered width and distance to human body	Effect of distance to human body

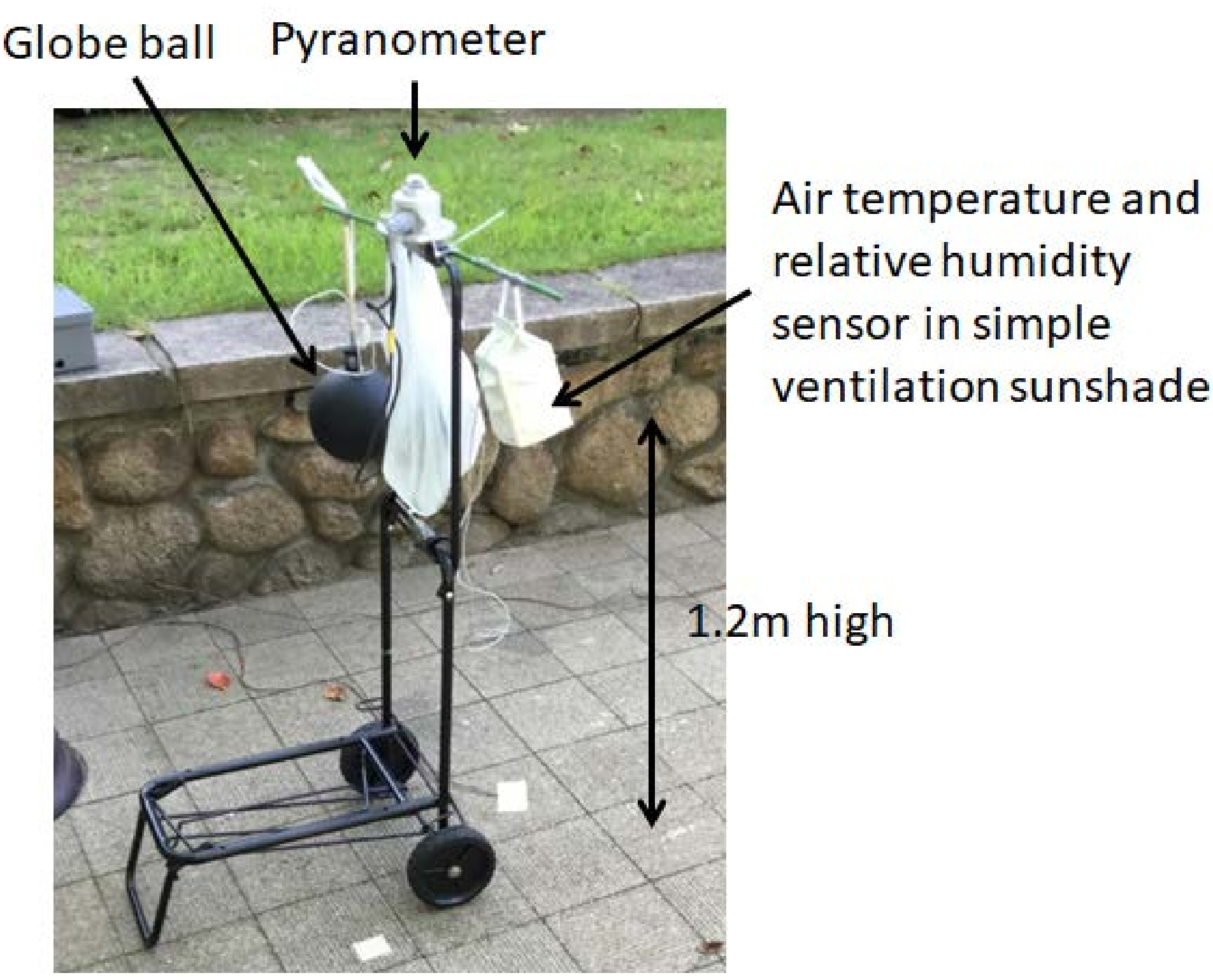
Globe ball
Pyranometer
Air temperature and relative humidity sensor in simple ventilation sunshade
1.2m high

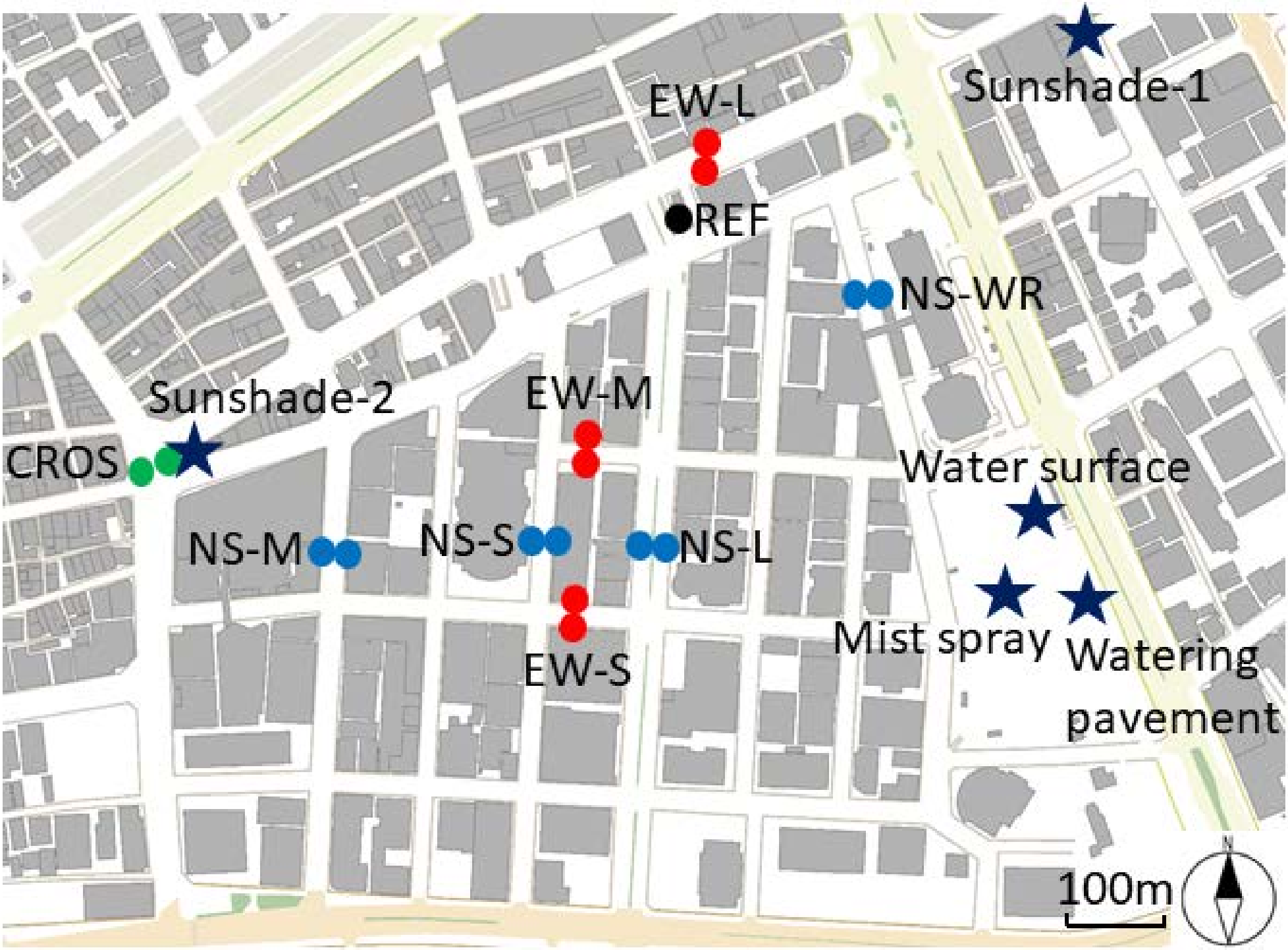

NS-L, -M, -S, -WR: North-south roads with large, medium, small road widths, water retention pavements

EW-L, -M, -S: East-west roads with large, medium, small road widths

CROS: Crossroad, REF: Reference,

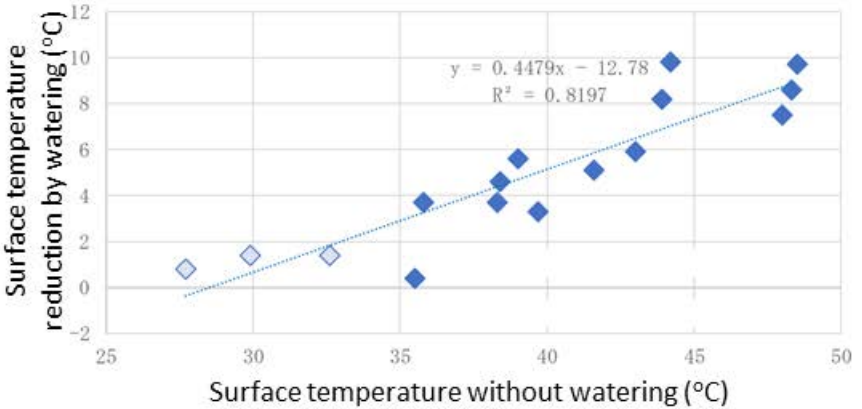

a. on north-south road immediately after watering

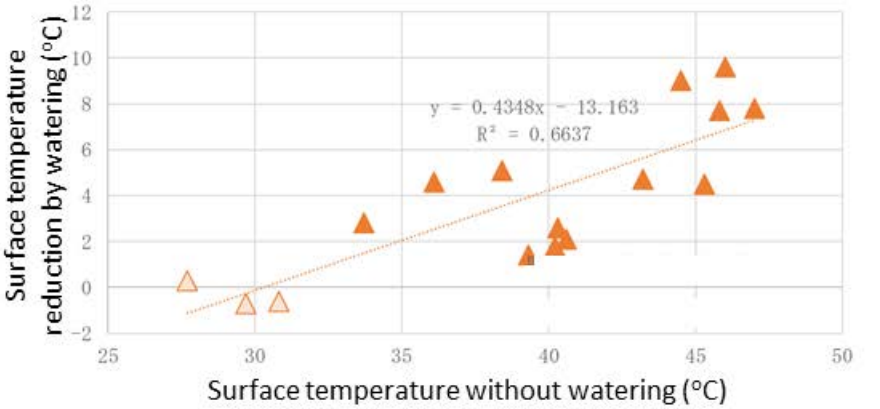

b. on north-south road 30 minutes after watering

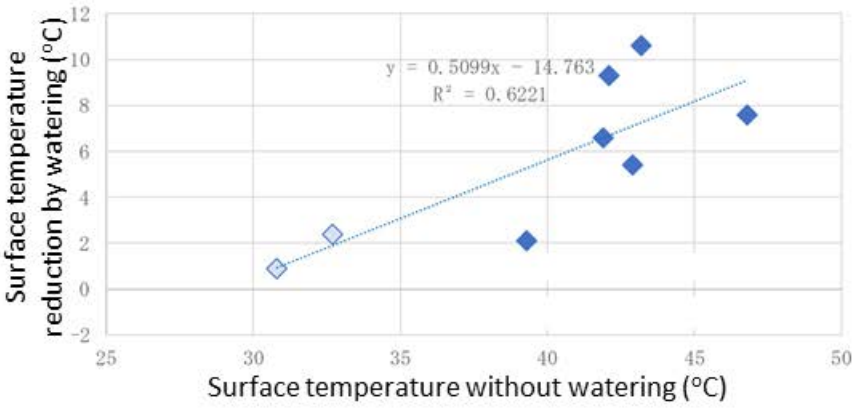

c. on east-west road immediately after watering

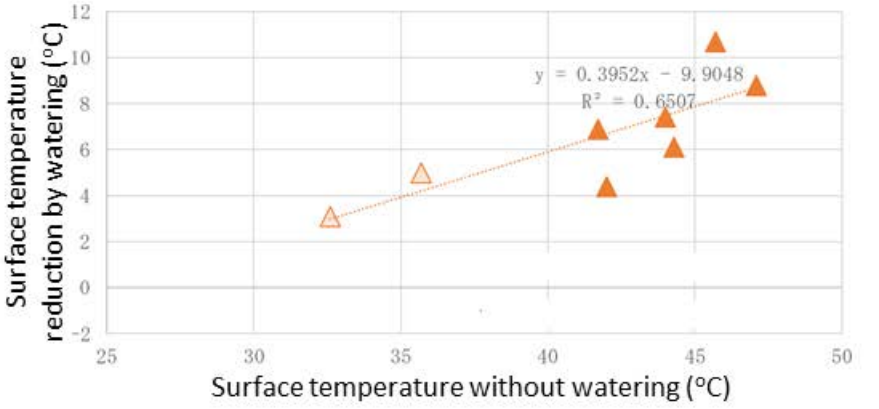

d. on east-west road 30 minutes after watering

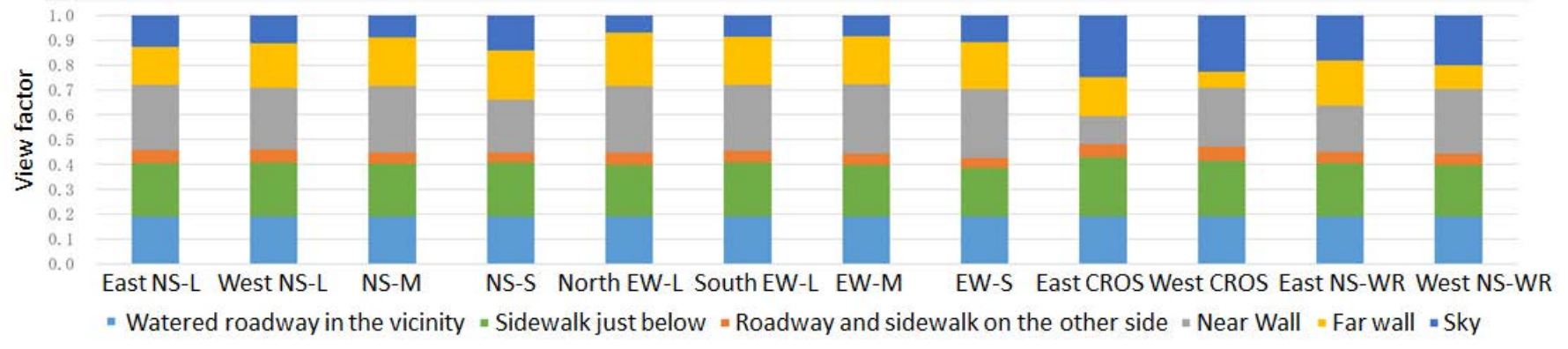
View factor
1.0
0.9
0.8
0.7
0.6
0.5
0.4
0.3
0.2
0.1
0.0
East NS-L
West NS-L
NS-M
NS-S
North EW-L
South EW-L
EW-M
EW-S
East CROS
West CROS
East NS-WR
West NS-WR
Watered roadway in the vicinity
Sidewalk just below
Roadway and sidewalk on the other side
Near Wall
Far wall
Sky

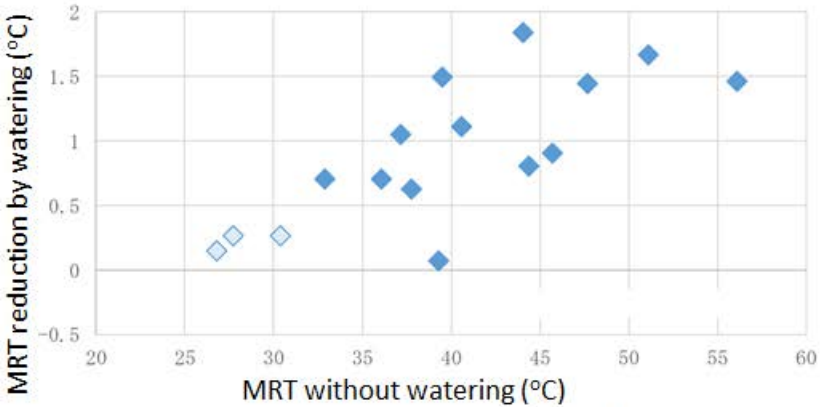

a. on north-south road immediately after watering

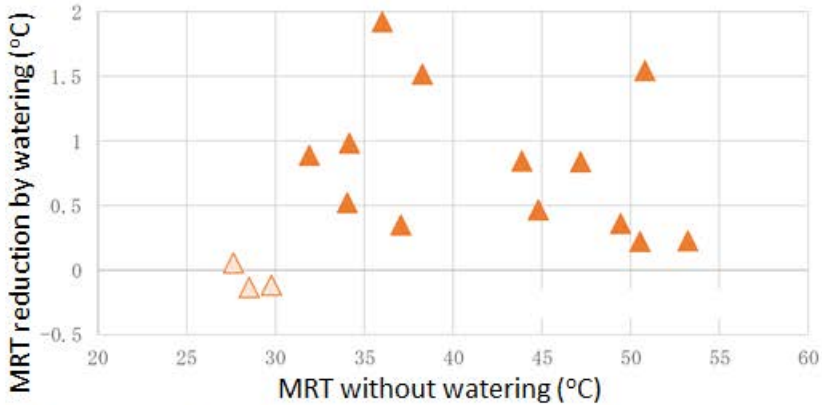

b. on north-south road 30 minutes after watering

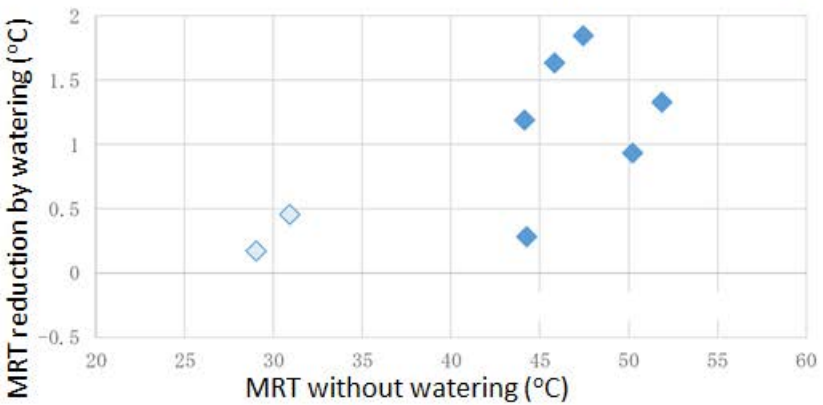

c. on east-west road immediately after watering

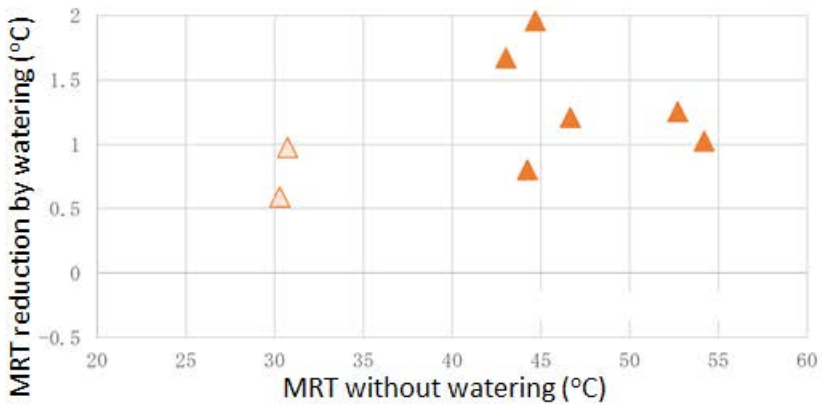

d. on east-west road 30 minutes after watering

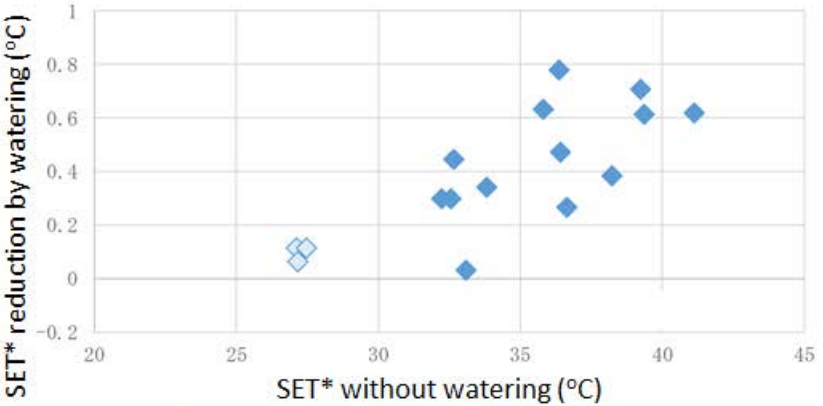

a. on north-south road immediately after watering

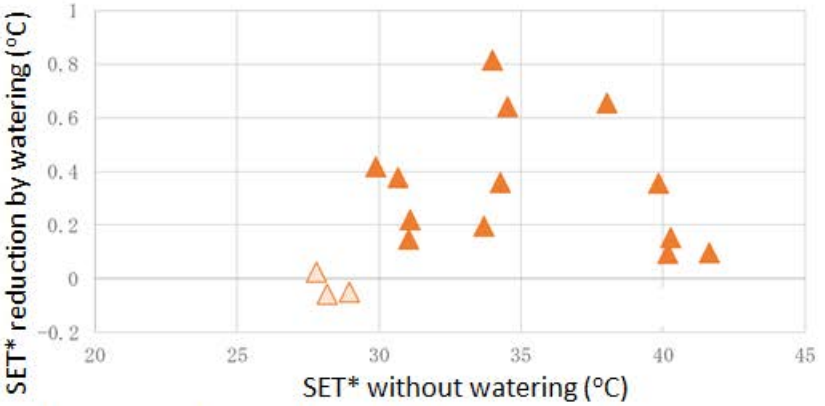

b. on north-south road 30 minutes after watering

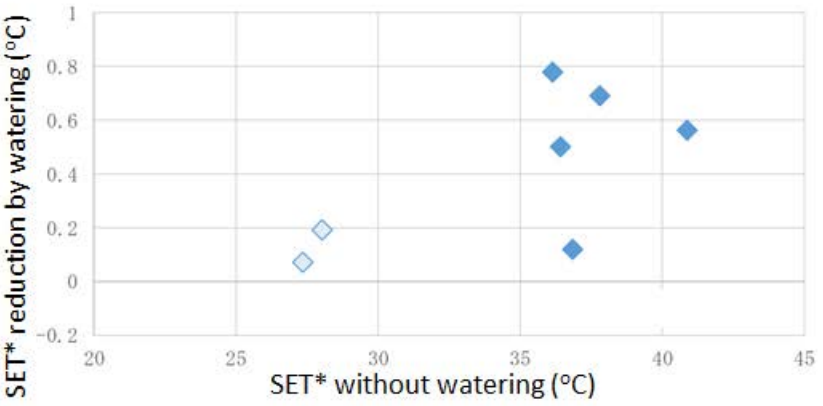

c. on east-west road immediately after watering

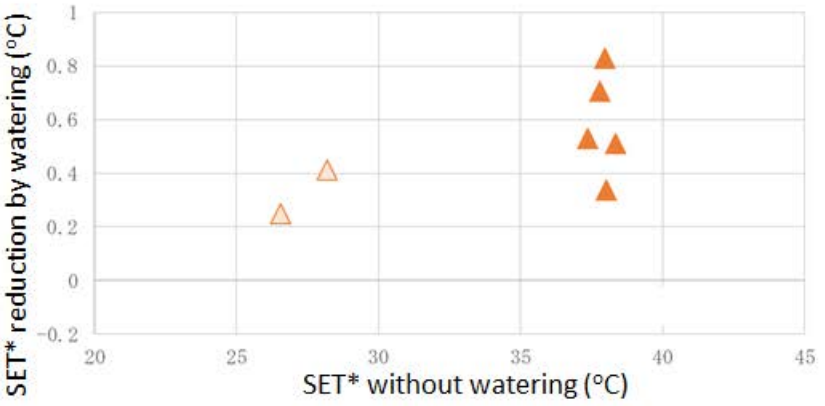

d. on east-west road 30 minutes after watering

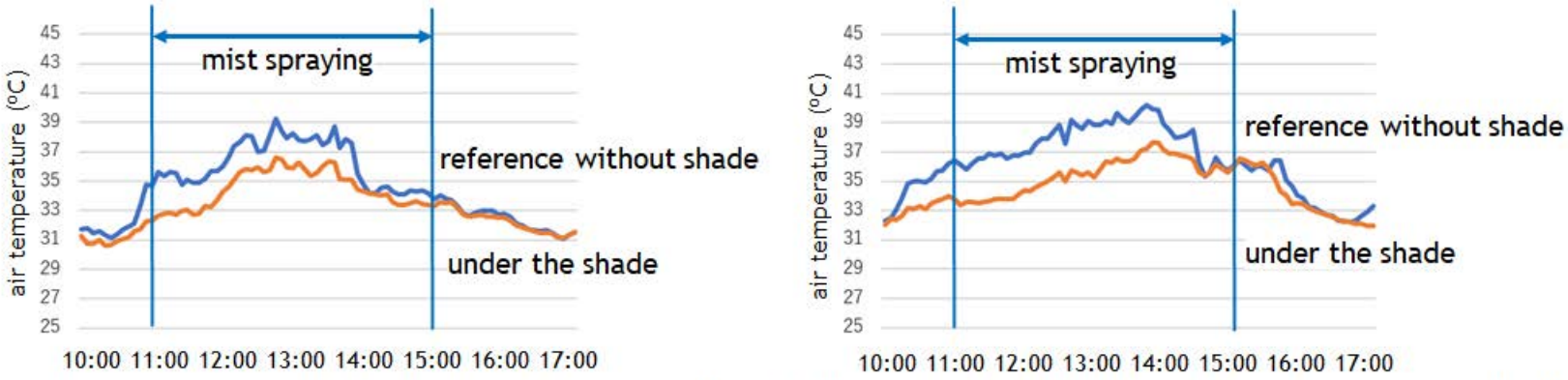

a. air temperature under the shade and reference without shade on July 30, 2019 (left: sunshade-1, right: sunshade-2)

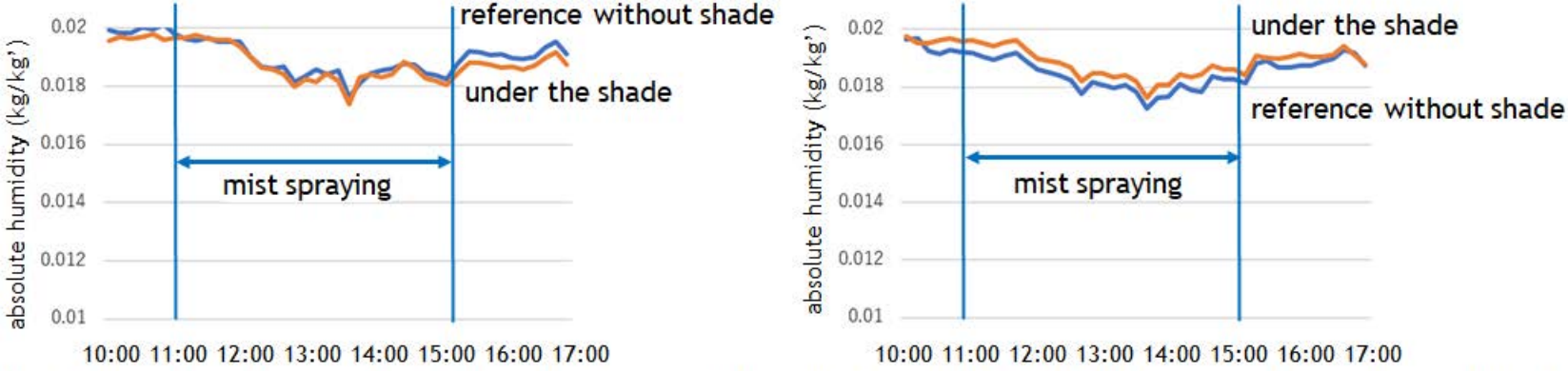

b. absolute humidity under the shade and reference without shade on July 30, 2019 (left: sunshade-1, right: sunshade-2)

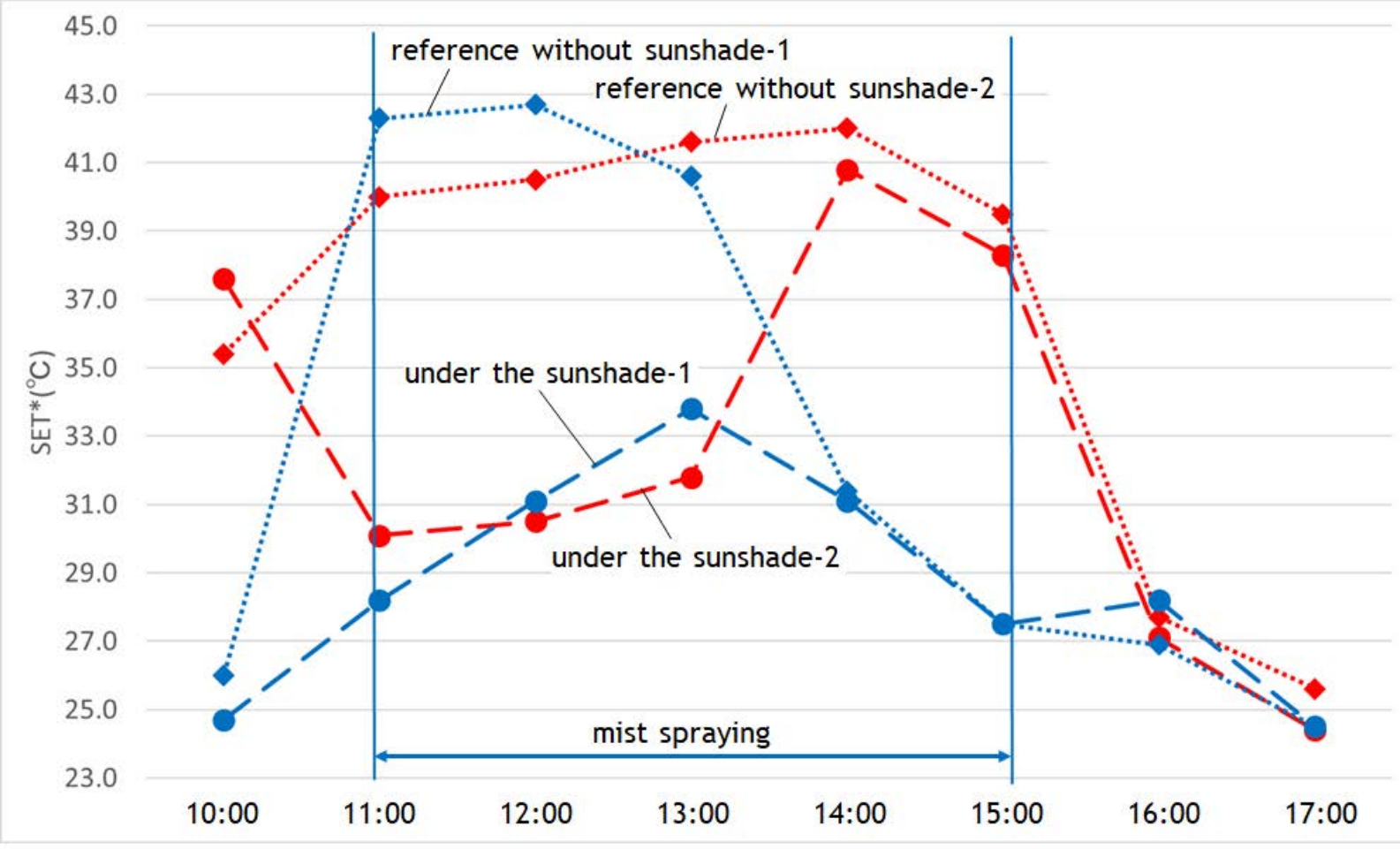
45.0
43.0
41.0
39.0
37.0
35.0
33.0
31.0
29.0
27.0
25.0
23.0
SET*(°C)
reference without sunshade-1
reference without sunshade-2
under the sunshade-1
under the sunshade-2
mist spraying
10:00
11:00
12:00
13:00
14:00
15:00
16:00
17:00

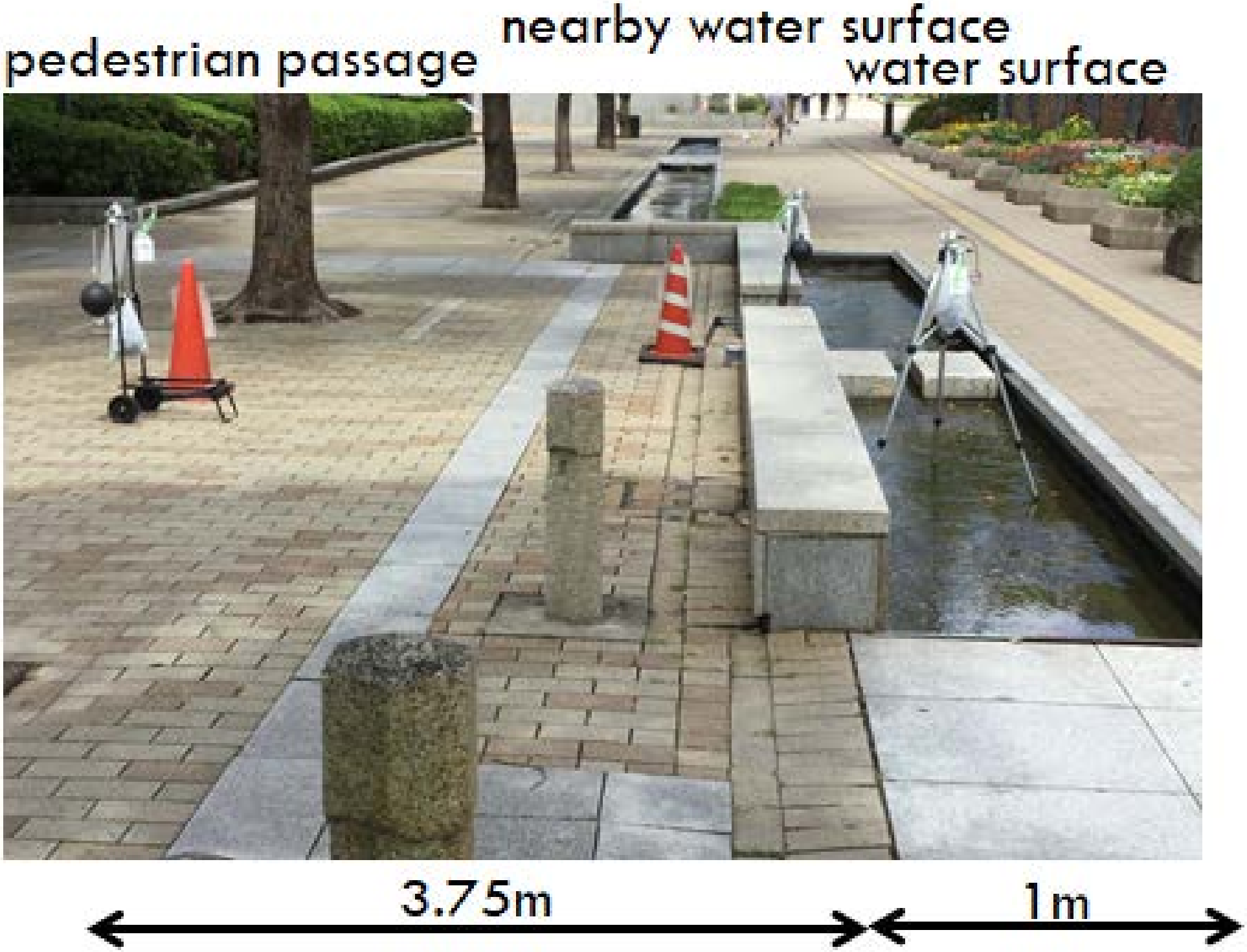
pedestrian passage
nearby water surface
water surface
3.75m
1m

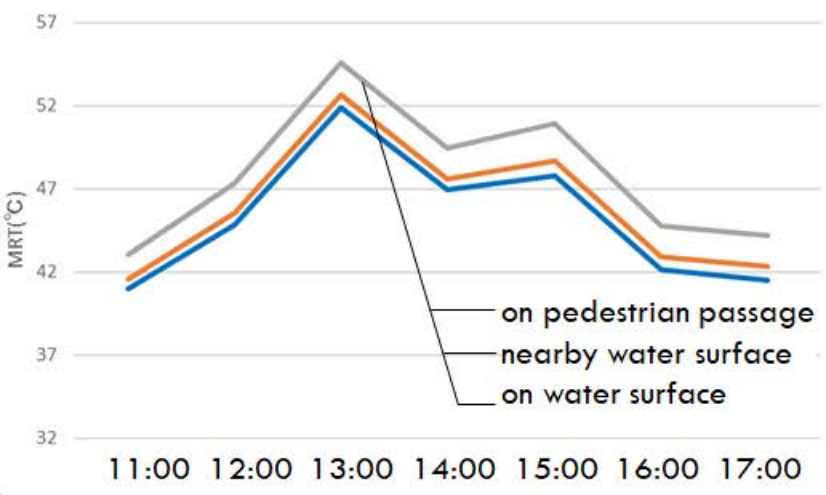
57
52
47
42
37
32
MRT(℃)
11:00
12:00
13:00
14:00
15:00
16:00
17:00
on pedestrian passage
nearby water surface
on water surface

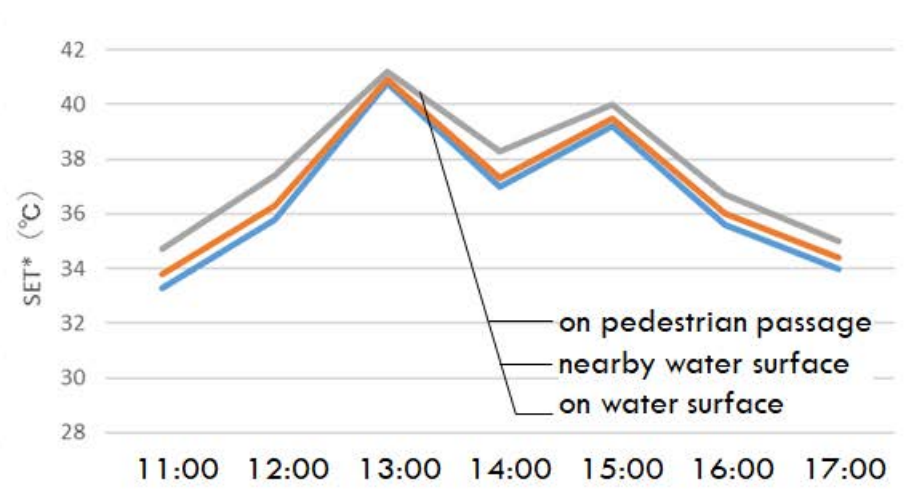
42
40
38
36
34
32
30
28
SET* (℃)
11:00
12:00
13:00
14:00
15:00
16:00
17:00
on pedestrian passage
nearby water surface
on water surface

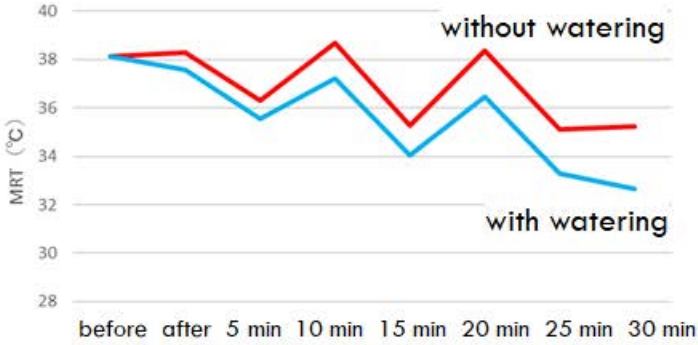

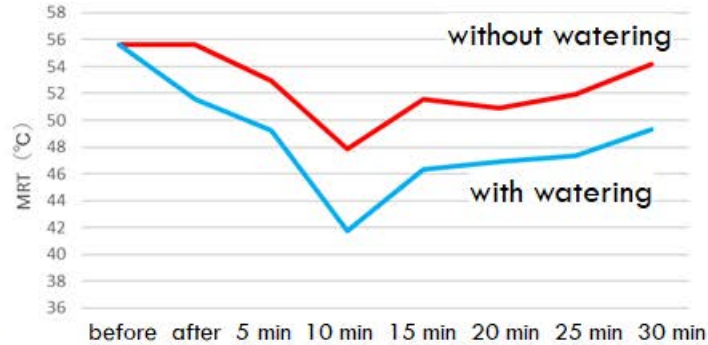

a. MRT before watering to 30 minutes after watering (left: watering at 8:00, right: watering at 14:00, on August 14, 2020)

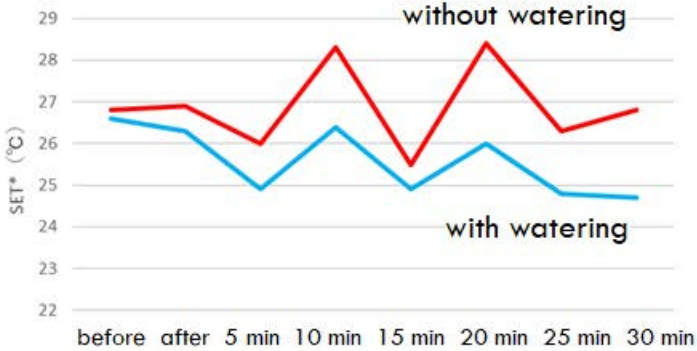

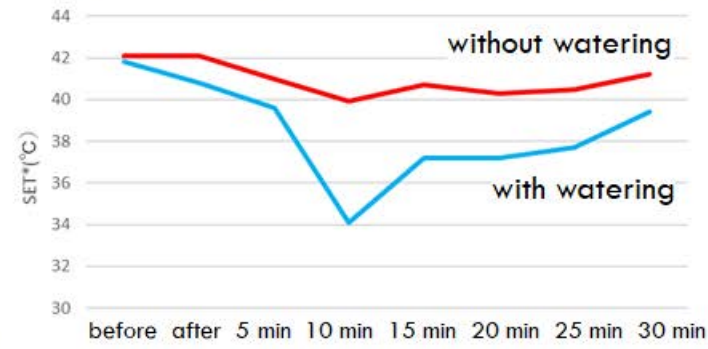

b. SET* before watering to 30 minutes after watering (left: watering at 8:00, right: watering at 14:00, on August 14, 2020)

mist outlet 1.3m above ground

a. sensors on 30 cm and 130 cm form mist outlet on tile surface

b. sensors on 30 cm and 230 cm form mist outlet on grass surface

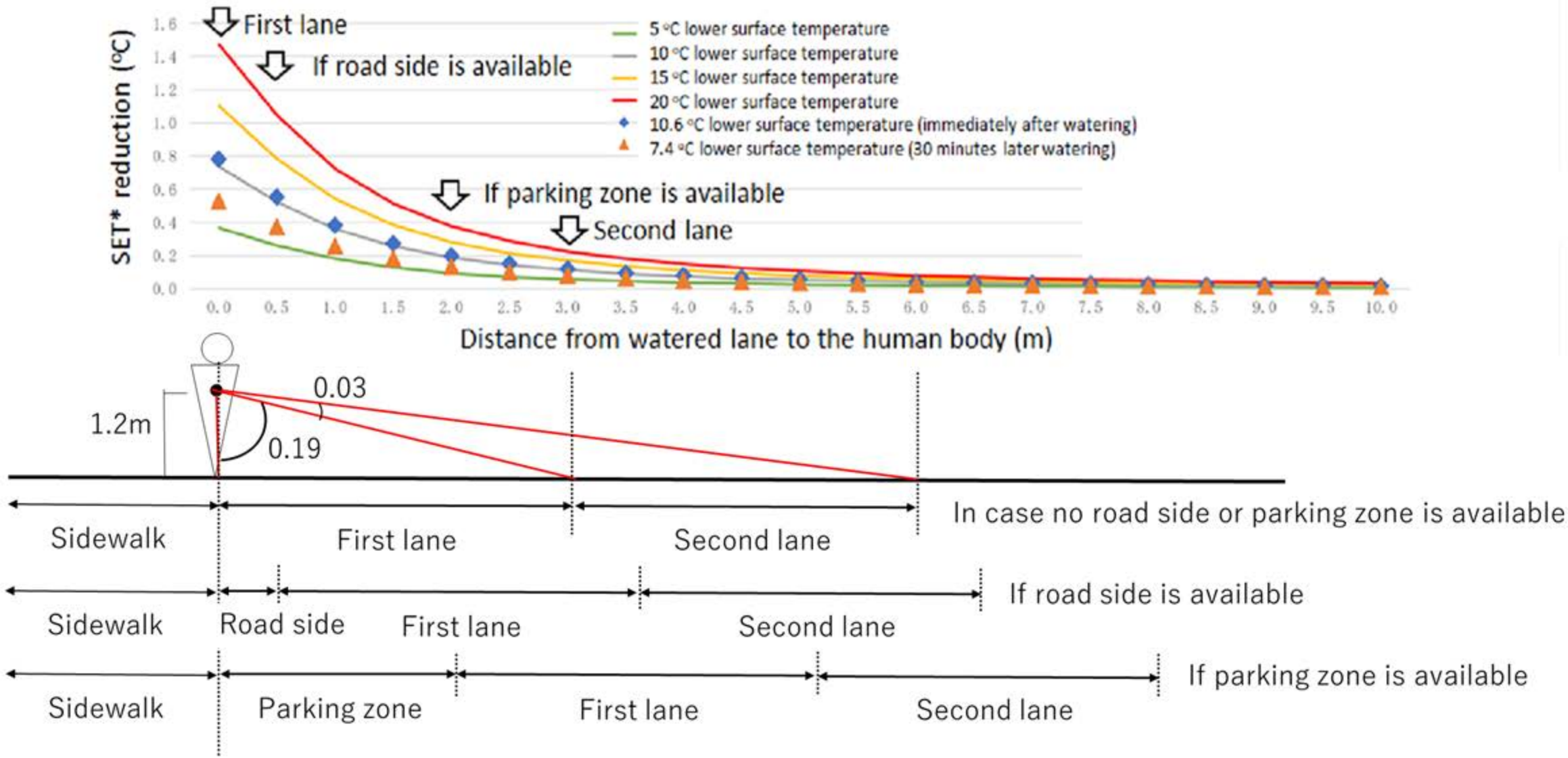
First lane
If road side is available
If parking zone is available
Second lane
5 °C lower surface temperature
10 °C lower surface temperature
15 °C lower surface temperature
20 °C lower surface temperature
10.6 °C lower surface temperature (immediately after watering)
7.4 °C lower surface temperature (30 minutes later watering)
SET* reduction (°C)
1.6
1.4
1.2
1.0
0.8
0.6
0.4
0.2
0.0
0.0 0.5 1.0 1.5 2.0 2.5 3.0 3.5 4.0 4.5 5.0 5.5 6.0 6.5 7.0 7.5 8.0 8.5 9.0 9.5 10.0
Distance from watered lane to the human body (m)
1.2m
0.03
0.19
Sidewalk
First lane
Second lane
In case no road side or parking zone is available
Sidewalk
Road side
First lane
Second lane
If road side is available
Sidewalk
Parking zone
First lane
Second lane
If parking zone is available

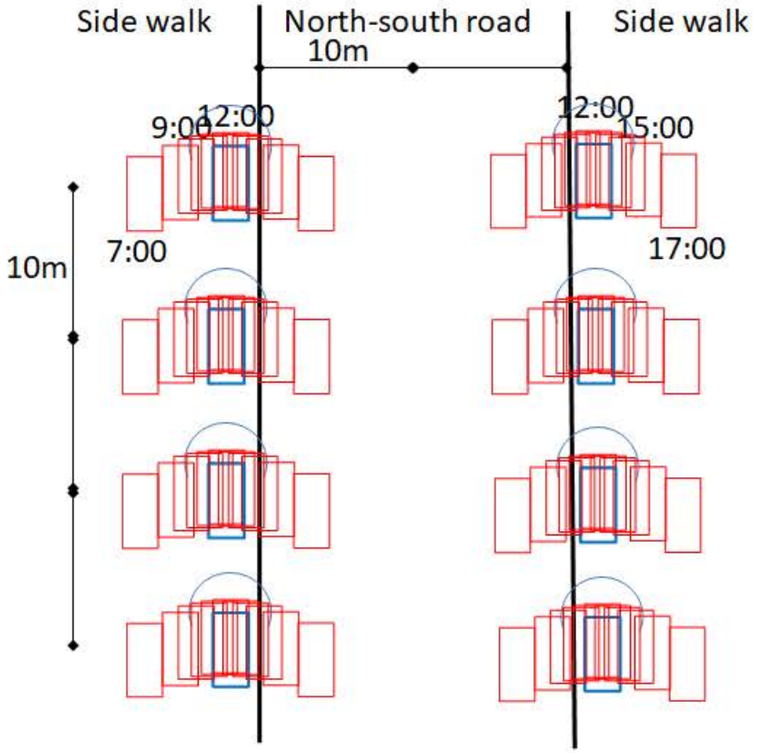

a. sunshade on the north-south road sidewalk

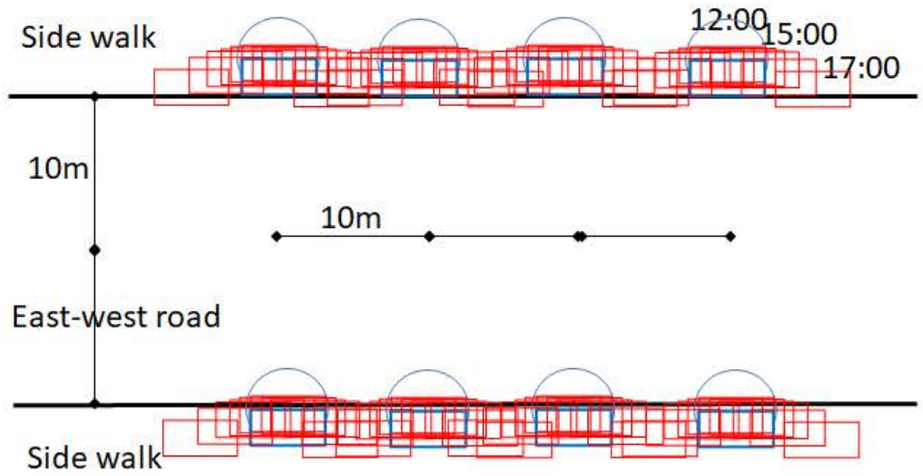

b. sunshade on the east-west road sidewalk

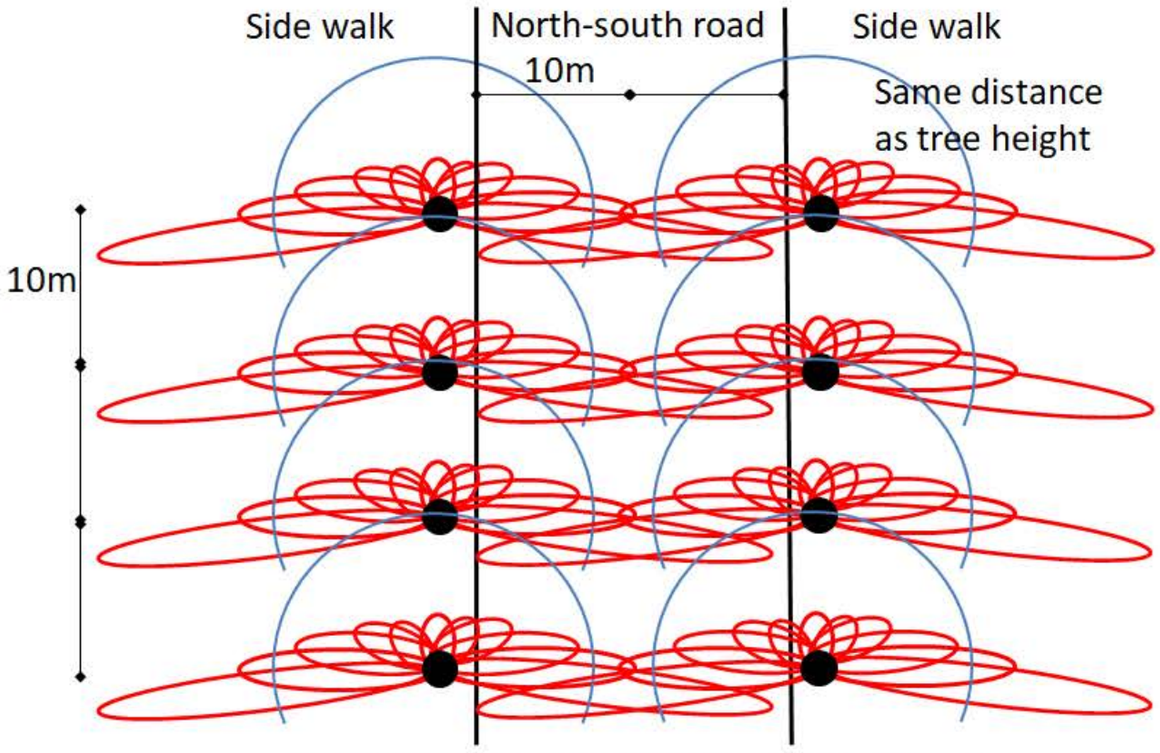

c. roadside tree on the east-west road sidewalk

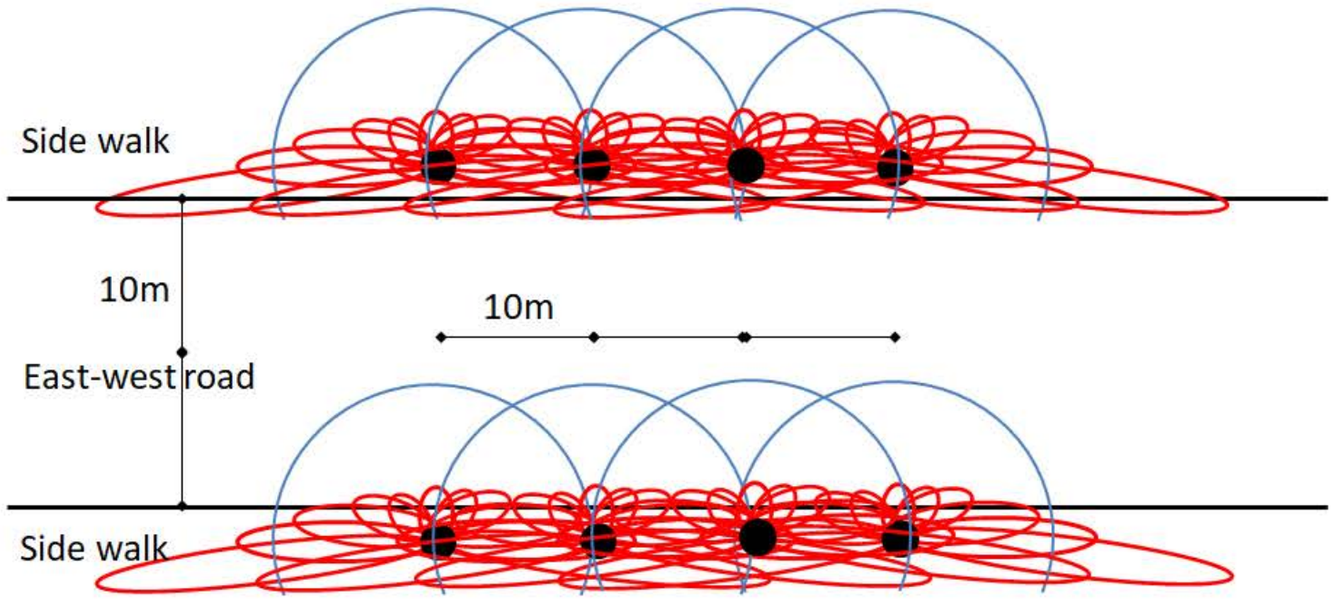

d. roadside tree on the north-south road sidewalk

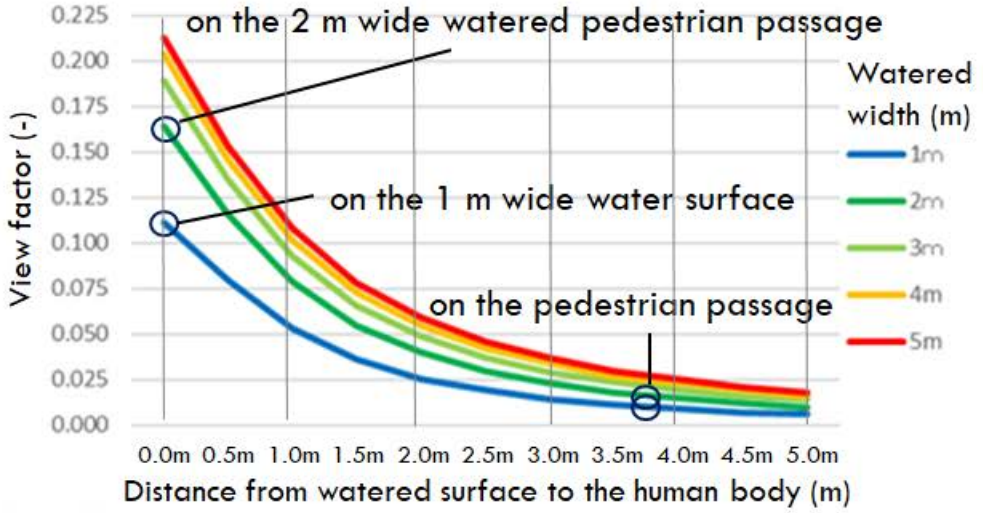

	view factor (-)	surface temperature reduction (°C)	MRT reduction (°C)
on the 1 m wide water surface	0.11	15	1.65
on the pedestrian passage 3.75 m away from 1 m wide water surface	0.011	15	0.17
on the pedestrian passage 3.75 m away from 2 m wide water surface	0.018	15	0.27
on the 2 m wide watered pedestrian passage	0.16	10	1.60